Polish J. Chem., **77**, 1547–1559 (2003)

Structure and Lattice Dynamics of $NH_4IO_3 \cdot 2HIO_3$ Crystal as Derived from IR, Raman and ^{127}I NQR Data*

by A. Barabash[1,2], J. Baran[3], T. Gavrilko[1], G. Puchkovskaya[1], H. Ratajczak[3] and Yu. Tarnavski[1]**

[1]*Institute of Physics, National Academy of Sciences of Ukraine, 46, Prospect Nauki, 03022 Kyiv, Ukraine*
[2]*Kyiv University of Economy and Technologies of Transport, 19, Lukashevich Str., 03049 Kyiv, Ukraine*
[3]*Institute of Low Temperature and Structure Research, Polish Academy of Sciences, 50-950 Wrocław, Poland*

(Received April 23rd, 2003; revised manuscript June 23rd, 2003)

The IR absorption and Raman spectra of $NH_4IO_3 \cdot 2HIO_3$ crystal (AIH) were reinvestigated in a wide temperature range (13–300 K), including the phase transition temperature T_c = 213 K. The pressure dependences of the quadrupole coupling constant e^2Qq_{zz} and asymmetry parameter η of electric field gradient tensor (EFGT) were obtained from the analysis of ^{127}I nuclear quadrupole resonance (NQR) spectra at 77 K. It was shown that the phase transition of the crystal can be described as an isostructural phase transition with ordering of protons in bifurcated hydrogen bonds and duplication of the unit cell.

Key words: NQR, vibrational spectroscopy, proton ordering, hydrogen bonds, lattice dynamics, superionic phase transition

The $NH_4IO_3 \cdot 2HIO_3$ crystal (AIH) is known as a proton conductor of conductivity $\sigma \sim 10^{-6}$ Om^{-1} cm^{-1} at room temperature. According to structural investigations of AIH crystal at 300 K [1–3], this crystal was assigned to triclinic system ($P\bar{1} = C_i^1$ space group) with two formula units per unit cell ($Z = 2$). On the basis of temperature studies of dielectric permittivity [1,2], it was shown that at T_c = 213 K the crystal undergoes a second-order phase transition into the superionic state. It was suggested that this superionic phase transition is connected with the ordering of protons in short hydrogen bonds. Following this suggestion, the crystal may exhibit ferroic properties at $T \leq T_c$. However, temperature investigations of macro parameters of the crystal did not reveal any polar properties in the low-temperature phase of the crystal [1]. Phase transition in the AIH crystal was also studied in [4–6] by spectroscopic and DSC methods, and a two-stage mechanism of the superionic conductivity in the crystals has been proposed. However, despite these numeric studies recently performed on AIH, the nature of the low-temperature phase and the mechanism of the phase transition in the crystal still remain unclear.

---

* Dedicated to Prof. M. Szafran on the occasion of his 70th birthday.

** Corresponding author. Tel.: (380-44) 265-15-52; Fax: (380-44) 265-15-89; E-mail address: puchkov@iop.kiev.ua

In this connection, we use temperature dependent IR, Raman and low-temperature NQR methods to verify the lattice dynamics and phase transition mechanism for the AIH crystal.

EXPERIMENTAL

Polycrystalline samples of AIH grown from an aqueous solution were used. The middle and far IR absorption spectra of the powdered crystal, suspended in Nujol and fluorolube, were recorded using the IFS-88 Bruker FTIR and FIS-3 Hitachi spectrometer in 380–4000 cm^{-1} and 400–100 cm^{-1} spectral range, respectively, with spectral resolution of 2 cm^{-1}. Temperature dependent IR spectra were measured between 13÷300 K, using an ADP cryogenics closed-cycle helium refrigerator system, which allowed to maintain the temperature of the sample constant to within ±0.1 K. Powder Raman spectra of AIH crystal were measured with DFS-24 spectrometer, using the 514.5 nm line of an argon ion laser. Temperature-dependent Raman study has been carried out between 77–300 K, using a continuous-flow cryostat system unit made in the Institute of Physics of NAS of Ukraine, equipped with an automatic temperature controller, which provided an accuracy of temperature stabilization of ± 0.5 K. The ^{127}I NQR spectra of the AIH crystal were investigated at 300 and 77 K with the help of a domestic IS-3 pulsed radiospectrometer. The precision of measurements for the NQR lines frequencies was ±10 kHz, and the accuracy of definition for the quadrupole coupling constant e^2Qq_{zz} and EFGT asymmetry parameter η amounted to ±0.01 MHz and 0.01%, respectively. The assignment of NQR lines to the two quadrupole transitions (1/2 → 3/2 and 3/2 → 5/2) was carried out using two-frequency technique. The pressure of $p \leq 0.4$ GPa was provided with the help of autonomic high-pressure hydraulic cell. Small quantity of alcohol was added to prevent crystallization of the transformer oil at low temperatures. The hydraulic properties of the mixture at 77 K were controlled by the width of ^{127}I NQR line of the AIH crystal.

RESULTS AND DISCUSSION

Vibrational spectra: The structure of the AIH crystal at 300 K was determined using neutron diffraction [3]. The AIH crystallizes in the triclinic space group crystal $P\bar{1} = C_i^1$ with two formula units in the crystallographic unit cell. The structure can be described as a framework of strongly distorted IO_6 octahedra, linked together by corner sharing and hydrogen bonds with NH_4^+ ions occupying the large cavities in this framework. The lattice parameters of AIH crystal in the high-temperature phase are as follows: $a = 0.8374(3)$, $b = 0.8311(3)$, $c = 0.8200(3)$ nm, $\alpha = 65.45(4)°$, $\beta = 59.96(4)°$, $\gamma = 70.15(4)°$ [1]. For 39 atoms per triclinic unit cell, the 114 vibrational degrees of freedom in the k = 0 limit are transformed according to the representation: $\Gamma = 51A_g + 57A_u$ (54 internal vibrations – $27A_g + 27A_u$, 24 librations – $12A_g + 12A_u$, and 36 translations – $15A_g + 21A_u$ including three acoustic modes $3A_u$). The results of factor group analysis and the correlation diagram are presented in Table 1. According to the results of the crystal structure studies [1–3], there are three crystallographically non-equivalent iodate ions in the structure of AIH connected by hydrogen bonds. The different structure of distorted iodate groups $I(1)O_3$, $I(2)O_3$ and $I(3)O_3$ is determined by the symmetry of their local surrounding in the crystal. There are three types of the O–H...O bonds and four types of weak N–H...O bridges in the crystal structure. The two oxygen atoms of $I(1)O_3$ groups form two hydrogen bonds O · · · H–N. Specific feature of the crystal structure is that $I(2)O_3$ and $I(3)O_3$ groups form infinite iodate cha-

ins, which are connected with each other in transversal directions by weak O···H–N bridges. The $I(2)O_3$ and $I(3)O_3$ groups are surrounded by one static O···H–N and two disordered or bifurcated hydrogen bonds O···H···O. It was shown that bifurcated hydrogen bonds are symmetric at 300 K. The structure fragments formed by iodate chains in the crystal at 300 K may be presented as follows:

…O*(22)–I*(2)–O*(23)···H(23)···O(23)–I(2)–O(22)…H(32)–
|
O*(21)…H–-NH_3…

O(21)…H–NH_3…

–O(32)–I(3)–O(33)···H(33)···O*(33)–I*(3)–O*(32)–H*(32)…
|
O(31)…H–NH_3…

O*(31)…H–NH_3…

Table 1. Correlation diagram for low temperature phase of $NH_4IO_3 \cdot 2HIO_3$ crystal.

Point symmetry of the ions	Site symmetry	Factor group symmetry
	NH_4^+	
T_d	C_1	C_i
ν_1 A (Raman)		
ν_2 E (Raman)	A	A_g (Raman)
		A_u (IR)
ν_3, ν_4 F_2 (Raman, IR)		
	IO_3^-	
C_{3v}	C_1	C_i
ν_1, ν_2 A_1 (Raman, IR)		
A_2 (Raman)	A	A_g (Raman)
		A_u (IR)
ν_3, ν_4 E (Raman, IR)		

According to [2], another specific feature of the high-temperature phase of AIH crystal is that the number of possible sites for the proton localization in the lattice exceeds the number of protons per unit cell. Presumably, this is responsible for mechanism of superionic conductivity of the crystal observed above 213 K.

Table 2 contains the vibrational frequencies observed at room temperature in the IR and Raman spectra of the AIH crystal. A symmetrical pyramidal IO_3^- belongs to the point group C_{3v}, and the four fundamental vibrational frequencies are expected in the IR absorption spectra at 779 (ν_3(E)), 625 (ν_1(A_1)), 360 (ν_1(A_1)) and 520 cm^{-1} (ν_4(E)) [7]. In the high-temperature phase of AIH crystal (above 213 K) practically all analyzed modes are reflected as diffused singlets in the IR and Raman spectra as a result of dynamic averaging of motions of all iodate anions in the lattice. On lowering the temperature, due to diminishing crystal symmetry restrictions (Table 1), the degeneracy of the asymmetric stretching fundamentals ν_3 and ν_4 is removed, and one can observe a rather complicated spectral profile in the region of internal vibrations of IO_3^- ions at around 800 cm^{-1} (Figs. 1–2), which is undoubtedly related to the existence of three non-equivalent IO_3 anions in this phase. The high-frequency spectral region (2000–4000 cm^{-1}) is characterized by absorption caused by NH and OH stretching vibrations (Fig. 3). The internal modes of undistorted NH_4^+ ion (assumed symmetry T_d) are expected at 3145 (ν_3(F_2)), 3040 (ν_1(A)), 1683 (ν_2(E)) and 1450 (ν_4(F_2)) cm^{-1}, among them only F_2 symmetry being active in IR absorption [7]. The spectra in the range of ammonium groups vibrations are not easily interpreted, because of overlapping of closely located bands of hydrogen bonds absorption and multiple Fermi-resonances. As it was shown in [8–9], the spectrum profile in the region of stretching NH vibrations of ammonia containing crystals is often complicated by the factor-group and resonance splitting of absorption bands, which is especially clearly manifested at low temperatures. According to [9], three bands with peak positions at 2837, 3040 and 3147 cm^{-1}, which are observed in the spectra of AIH crystal at 300 K, originate from complex multi-mode Fermi-resonance between the ν_1(A) fundamental of NH_4^+ ion and the second harmonics: $2\nu_4$(F_2) and ν_2(E) + ν_4(F_2) (see Table 2). Furthermore, the IR absorption spectra of the AIH crystal show bands with the peak positions at 3047 and around 1660 cm^{-1}. These bands are assigned to ν_1(A_1) and ν_2(E) vibrations of NH_4^+ ion which, according to factor-group analysis are forbidden in the IR spectra for undistorted tetrahedral NH_4^+ ion, but are allowed for the distorted NH_4^+ ion of C_1 symmetry in the triclinic crystal lattice. At the lowest temperatures, all these bands are sharpen, and the width of all of them decrease significantly, due to a substantial change in the motional state of ammonia cations (Fig. 3). The multiplicity of the NH stretching and bending modes below 213 K in the spectra of AIH crystal may indicate "freezing" of the rotation of NH_4^+ cations or, more probably, the non-equivalence of the cations. It should be also noticed that the NH stretching vibrations are not very sensitive to the phase transition, and so weak NH..O hydrogen bonds do not contribute to the mechanism of this phase transition.

Table 2. Frequencies and assignment of the observed modes to the respective vibrations for the high-temperature phase of $NH_4IO_3 \cdot 2HIO_3$ crystal (T = 300 K).

IR frequency, cm^{-1}	Raman frequency, cm^{-1}	Assignment
3220		$\nu_3(F_2)$ (NH_4^+)
3147		$\nu_2 + \nu_4$ (NH_4^+)
3040	3061	$\nu_1(A)$ (NH_4^+)
2837	2839	$2\nu_4$ (NH_4^+)
2800		$\nu_1(OH)$
2587	2371	$\nu_2(OH)$
2280	2300	$\nu_3(OH)$
	1673	
1667		$\nu_2(E)$ (NH_4^+)
1663		
1420	1433	$\nu_4(F_2)$ (NH_4^+)
1233		$\delta_3(OH)$
1200		
1124		$\delta_2(OH)$
1097		$\delta_1(OH)$
1071		
889		
820	825	
790	806	
	767	$\nu_3(E)$ (IO_3^-)
757	756	
697	689	$\nu_1(A_1)$ (IO_3^-)
663	657	
629		
398	401	$\nu_6(A)$
379	374	
334		$\nu_2(A_1)$ (IO_3^-)
318	329	$\nu_4(E)$ (IO_3^-)
288	305	
	235	
199	214	
154	157	
113	107	
	94	Lattice vibrations
	78	
	57	

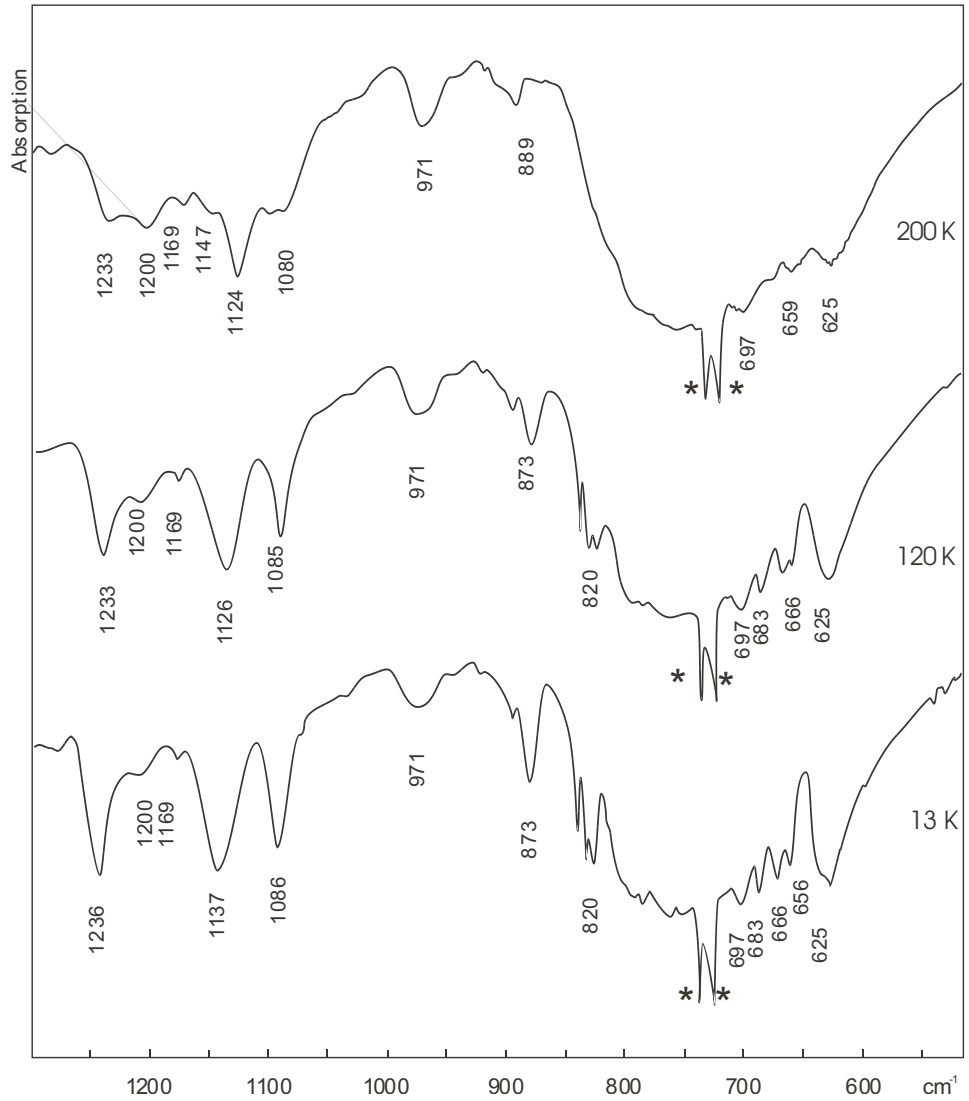

Figure 1. FTIR absorption spectra of AIH crystal in the region of ν(IO) and δ(OH) vibrations at different temperatures. Asterisks denote the Nujol absorption bands.

Consider another three crystallographically non-equivalent types of bifurcated O–H…O hydrogen bonds in the high-temperature phase of AIH crystal. We have estimated the peak positions of OH stretching bands in IR spectra using well-known Novak's correlation [10] between the ν(OH) frequencies and the $R_{O...O}$ distance. The lengths of three O–H...O bonds in the AIH crystal, as reported in [2], are 2.591, 2.576, and 2.567 Å, respectively, and, therefore, they can be attributed to medium-strong hydrogen bonds. It is known [10–11] that the formation of medium strong hydrogen bonds results in the appearance of an intensive broad ν(OH) stretching band in the region of 2800–2200 cm^{-1}. Presumably, the broad bands of medium intensity centered at 2800, 2587 and 2280 cm^{-1} in the AIH spectra at T = 300 K may be assigned to ν(OH)

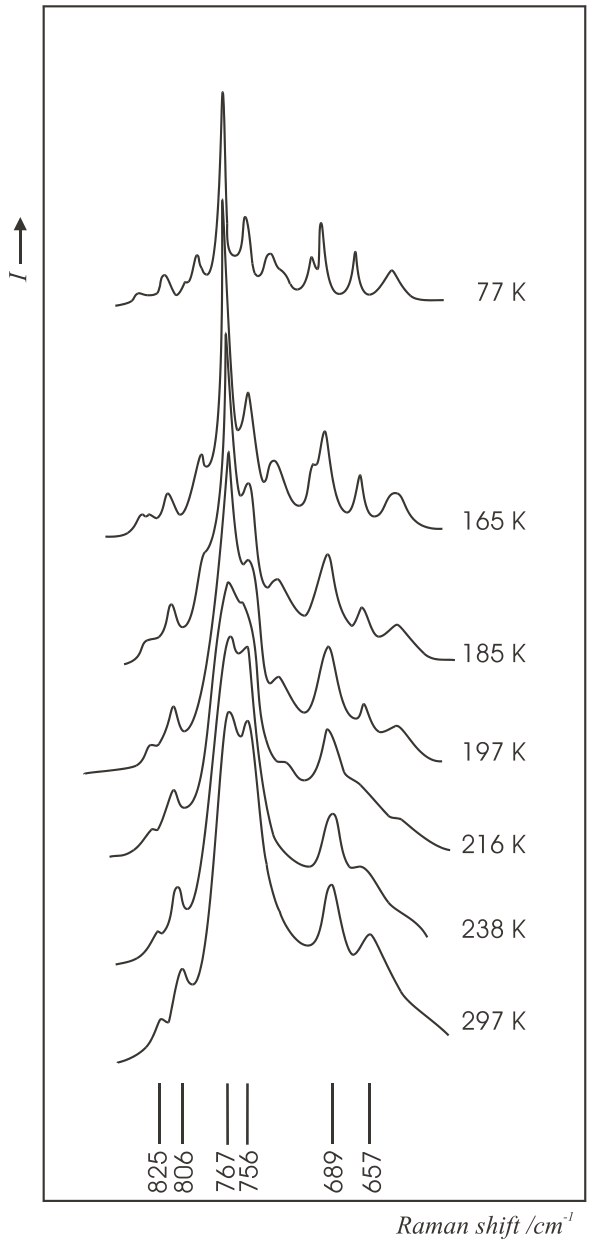

Figure 2. Powder Raman spectra of AIH crystal in the region of ν(IO) stretching vibrations at different temperatures.

stretching vibrations of three different bifurcated OH…O hydrogen bonds. It is worth mentioning that small intensity of OH stretching vibrations is characteristic of symmetric hydrogen bonds. Correspondingly, the existence of three types of H-bonds in the AIH crystal gives rise to the three in-plane bending δ(OH) vibrations, which are clearly observed at the frequencies 1080, 1124 and 1233 cm^{-1}.

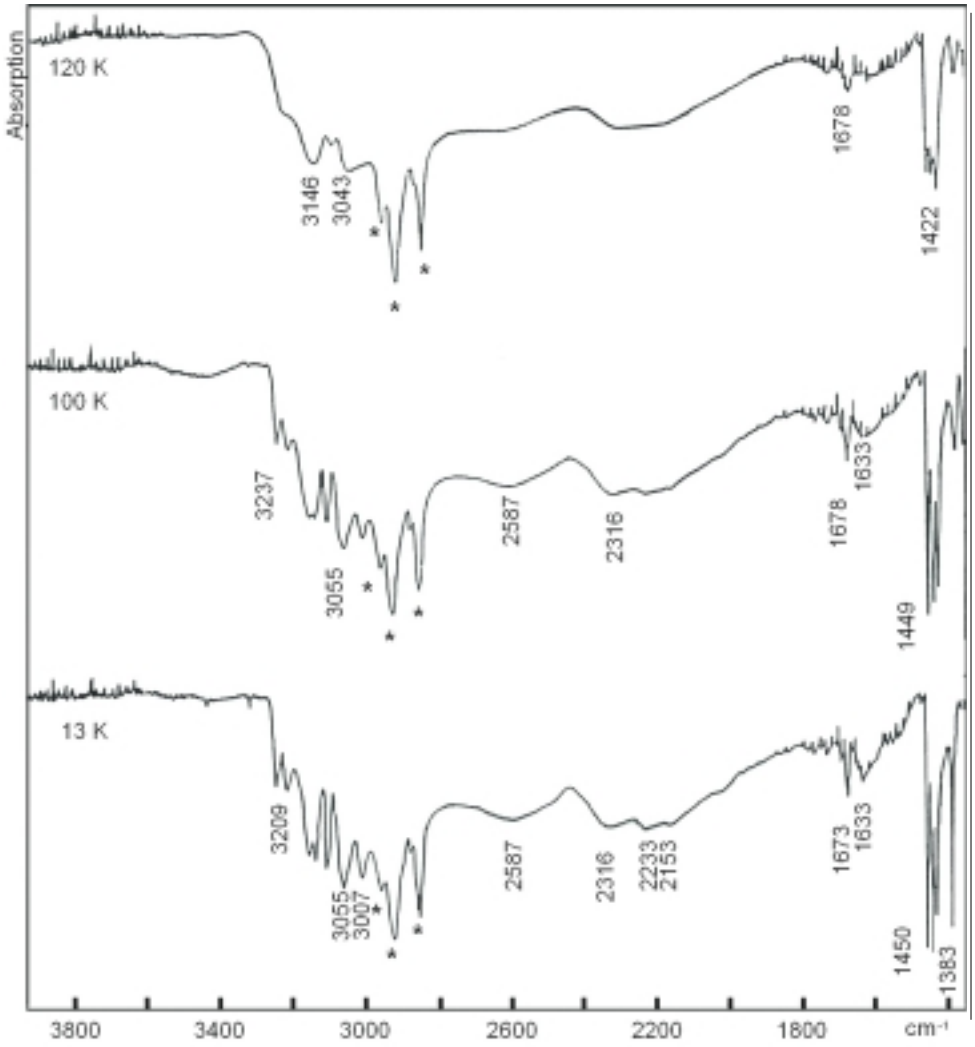

Figure 3. FTIR absorption spectra of AIH crystal in the region of ν(NH) and ν(OH) vibrations at different temperatures. Asterisks denote the Nujol absorption bands.

In the spectra of low-temperature phase (below T_c) of the AIH crystal (Fig. 3), only small changes in the high-frequency region of OH stretching vibrations can be seen, which are known to be the most sensitive to phase transitions in protonic subsystem and variation of crystal structure. Small changes are observed in the region of δ(OH) bending vibrations, which may be generally characterized as anticipated changes, related to narrowing of all the bands and growing of their intensities. The increase of the frequencies of bending δ_2(OH) and δ_3(OH) vibrations by 5 to 10 cm^{-1} indicates the strengthening of OH…O interactions as a result of shortening of the O…O distance. So, the structural phase transition entailing ordering of protons on bifurcated hydrogen bonds is hardly visible in the IR spectra. The characteristic feature of analyzed low-frequency Raman spectra of AIH crystal is a drop of overall intensity

of the spectra when the phase transition is crossed [4], while the spectra then again ignites at T = 77 K. It implies the decrease in the overall polarizability of the crystal at temperatures below T_c. At the same time, the phase transition in AIH is noticed as a change in the slope of the plots of intensity *versus* temperature for the IR absorption band centered at 99 cm^{-1} (Fig. 4) and 756 cm^{-1} line in the Raman spectra (Fig. 5). This suggests drastic changes in the dynamics of anionic sublattice, which can be caused by modification of local surrounding of iodate pyramidal ions. Summarizing, spectroscopic data of AIH crystal give evidence for an iso-structural phase transition, *i.e.* the AIH crystal retains its symmetry above and below T_c. Spectroscopic behavior of stretching and bending vibrations of hydrogen bonds change only slightly. It should be mentioned, that similar features are characteristic of other iodates with order-disorder phase transitions, where the second order phase transition has been seen in the IR spectra only as changes in slopes of the temperature dependence of OH bending frequency [12]. This implies, that to verify the postulated proton ordering, we should use other methods, such as for example NQR technique, which is known to be very sensitive to detect even insignificant changes in a crystal structure.

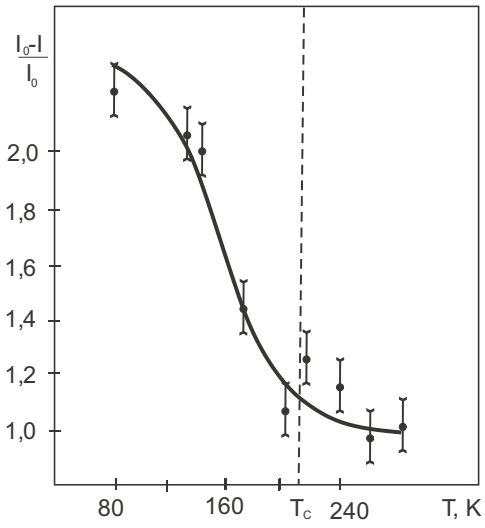

Figure 4. Variation of the peak intensity of 99 cm^{-1} band in the FIR absorption spectra of the AIH crystal *vs*. temperature.

NQR results: The existence at 300 K of three kinds of non-equivalent iodate groups should result in the multiplicity of the ^{127}I NQR spectra of AIH crystal, namely its NQR spectrum should consist of three lines. Though in the NQR spectra of high-temperature phase, these three lines are hardly visible, due to dynamic state of IO_3^- and NH_4^+ ions. As it follows from the analysis of the crystal symmetry, in the low-temperature phase (below T_c) the ^{127}I NQR spectra should consist of six lines [13]. Such multiplicity of NQR spectra (Table 3) can be explained by the destruction of bifurca-

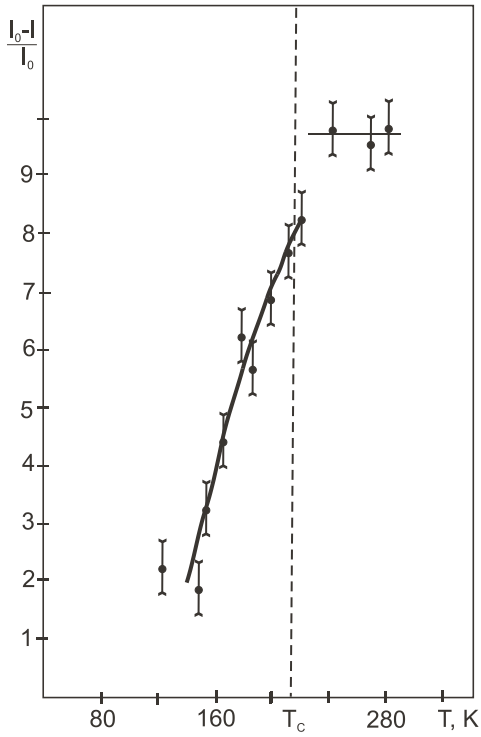

Figure 5. Variation of the peak intensity of 756 cm^{-1} band in the Raman spectra of the AIH crystal *vs*. temperature.

ted hydrogen bonds, which became asymmetric at $T < T_c$. In this case (at $T < T_c$) each of the three NQR lines, which are observed at 300 K, should split into two lines. This follows from the analysis of the structure of iodate chains in the AIH crystal at 77 K, when the protons occupy the asymmetric positions in bifurcated hydrogen bonds. The structures of the chains with ordered protons can be presented as follows:

$$\begin{array}{l} -H_1(23)\ldots O_1(23)-I_1(2)-O_1(22)\ldots H_1(32)- \\ \qquad\qquad\qquad\qquad\quad | \\ \qquad\qquad\qquad\qquad O_1(21)\ldots H-NH_3\ldots \end{array}$$

$$\begin{array}{l} \ldots H_2(23)-O_2(23)-I_2(2)-O_2(22)\ldots H_2(32)- \\ \qquad\qquad\qquad\qquad\quad | \\ \qquad\qquad\qquad\qquad O_2(21)\ldots\ H-NH_3\ldots \end{array}$$

$$\begin{array}{l} \ldots H_1(32)-O_1(32)-I_1(3)-O_1(33)\ldots H_1(33)- \\ \qquad\qquad\qquad\qquad\quad | \\ \qquad\qquad\qquad\qquad O_1(31)\ldots\ H-NH_3\ldots \end{array}$$

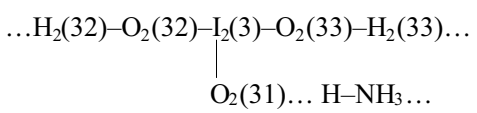

Table 3. Parameters of the ^{127}I NQR spectra of the low-temperature phase of $NH_4IO_3 \cdot 2HIO_3$ crystal (T = 77 K).

	$\nu_{1/2-3/2}$, MHz	$\nu_{3/2-5/2}$, MHz	e^2Qq_{zz} MHz	η, %
1	156.25	309.46	1033.12	8.70
2	157.05	312.65	1042.93	5.98
3	159.32	309.53	1036.51	15.12
4	180.41	330.62	1117.66	26.92
5	173.78	318.63	1077.25	26.83
6	202.24	320.15	1109.71	46.86

The assignment of the six lines, observed at $T \leq T_c$ in the ^{127}I NQR spectra of the crystal, to different fragments of iodate chains can be made following the analysis of pressure dependences of the NQR spectra parameters. The pressure dependences $e^2Qq_{zz}(p)$ and $\eta(p)$ were interpreted in terms of the behavior of hydrogen contacts O···H–O and O···H–N in the field of increasing hydrostatic pressure. As it has been reported in [13], there exists an empirical correlation between the length of covalent bond r(O–H) and the length of hydrogen bridge R(O···O) in H-bonded crystals, which has the form of inverse relationship r(O–H) ~ $R(O \cdots O)^{-1}$. Therefore, if R decreases with pressure, the length of covalent bond r increases. This means, that under the hydraulic pressure the proton in the hydrogen bridge should move towards the center of this bridge and therefore, the hydrogen bridge becomes more symmetric. Similar behavior was observed in [14] for α-$KIO_3 \cdot HIO_3$ crystal. The pressure coefficients $(1/q_{zz}^0)(dq_{zz}/dp)$ and $(1/\eta^o)(d\eta/dp)$ measured in [14] for $I^{127}(1)$ and $I^{127}(2)$ presents different signs, as it was expected from the empiric correlation. So, the analysis of the values of asymmetry parameters $\eta(p)$ of different NQR lines and their pressure coefficients $(1/q_{zz}^0)(dq_{zz}/dp)$ and $(1/\eta^o)(d\eta/dp)$, allow us to make an assignment of the six NQR lines, observed for AIH crystal. Using the data from [15], we calculated the asymmetry parameter η of the electric field gradient tensor and the quadrupole coupling constant e^2Qq_{zz} for different lines of multiple NQR spectra at variable hydrostatic pressures (Table 4). As it is seen from the Table 4, for the first two NQR lines, the coefficient η has the smallest value and increases with pressure. Therefore, these two lines can be assigned to $I_{1,2}(1)O_3$ groups, forming two weak hydrogen bonds O···H–N. The asymmetry parameter $\eta(p)$ obtained for the third NQR line has a larger value and shows similar behavior with pressure, thus, suggesting that it is associated with $I_1(2)O_3$ group involved in stronger hydrogen bonds O…H–O and O…H–N.

Table 4. The pressure coefficients for the pressure dependences $e^2Qq_{zz}(p)$ and $\eta(p)$ and assignment of the NQR lines of the low-temperature phase of $NH_4IO_3 \cdot 2HIO_3$ crystal (T = 77 K).

	e^2Qq_{zz}, MHz	η, %	$(1/q^o_{zz})(dq_{zz}/dp)$ 10^3, kbar^{-1}	$(1/\eta^o)(d\eta/dp)$ 10^3, kbar^{-1}	Assignment
1	1033.12	8.70	0.9	16.2	...H–N
2	1042.93	5.98	0.9	14.6	$I_{1,2}(1)O_3$ ...H–N
3	1036.51	15.12	1.1	13.0	...H–N $I_1(2)O_3$...H–O ...H–O
4	1117.66	26.92	–	–	–H...O $I_2(2)O_3$...H–O ...H–N
5	1077.25	26.83	–0.2	–9.9	–H...O $I_1(3)O_3$...H–O ...H–O
6	1109.71	46.86	1.0	–0.2	–H...O $I_2(3)O_3$–H...O ...H–N

The NQR lines, having negative pressure coefficients $(1/q^0_{zz})(dq_{zz}/dp)$ and $(1/\eta^o)(d\eta/dp)$ (Table 4, lines 5 and 6) were assigned to $I_1(3)O_3$ and $I_2(3)O_3$ groups. The $I_1(3)O_3$ is involved in two hydrogen bonds O…H and one covalent O–H bond, whereas $I_2(3)O_3$ group is linked with two covalent bonds O–H and one hydrogen bond O...H–N. It should be mentioned that due to a small signal-to-noise ratio we could not measure the pressure dependence of $e^2Qq_{zz}(p)$ and $\eta(p)$ for the forth NQR line. The assignment of this NQR line to $I_2(2)O_3$ group was made by the analogy with the fifth NQR line, having the close value of the pressure coefficient $\eta(p)$.

Since the structure of the high-temperature phase of AIH crystal implies, that the centers of symmetry should be located at geometrical center of bifurcated hydrogen bonds [2], the assumed model of the phase transition must result in the lost of the symmetry center in the low-temperature phase. However, as we have already noted, no ferroelectric properties were detected for the AIH crystal at $T < T_c$: neither domain structure of the crystal nor hysteresis loops were observed [1]. These experimental facts can be explained as arising from an antipolarity in the crystal structure at $T < T_c$ accompanied by duplication of the crystal unit cell. As the result, the crystal symmetry remains unchanged. The scheme of the phase transition may be written as follows:

$$C^1_i(Z = 2) \overset{T_c}{\Rightarrow} 2[C_i(Z = 2)] \equiv C^1_i(Z = 4).$$

Taking into account the multiplicity of the NQR spectra, which was observed in the low-temperature phase of AIH crystal, it seems reasonable to suppose that the mechanism of the superionic phase transition in the AIH crystal can be considered as follows: due to protons ordering, the doubling of the unit cell of the crystal takes place at

temperature $T_l < T_c$, and the IO_3^- anions become crystallographically non-equivalent in the low temperature phase. However, the role of anionic subsystem in the sequence of phase transitions in the crystal is not completely clear, due to the lack of information about the crystal structure at lower temperatures. Therefore, the superionic phase transition in the AIH crystal requires further investigation by other techniques.

CONCLUSIONS

Summarizing, complex spectroscopic and pressure dependent ^{127}I NQR studies were found to be a useful tool in studies of phase transitions in hydrogen-bonded AIH crystal. An interpretation of NQR lines was made in terms of pressure behavior of hydrogen bonded systems. It was concluded that the phase transition ($T_c = 213$ K) in the AIH crystal is an isostructural one and it is connected with destruction of bifurcated hydrogen bonds, which became asymmetric below the phase transition temperature. The postulated phase transition mechanism, which suggested proton ordering at T_c accompanied with duplication of crystal unit cell, while retaining the crystal symmetry, is consistent with FTIR and Raman spectroscopic data.

Acknowledgment

The authors thank Dr. K. Eshimov (Samarkand State University) for measurements of FIR spectra.

REFERENCES

1. Baranov A.I., Dobrzhansky G.F., Ilyukhin V.V., Kalinin V.P., Ryabkin V.A. and Shuvalov L.A., *Kristallografiya*, **24**, 280 (1979).
2. Baranov A.I., Dobrzhansky G.F., Ilyukhin V.V., Ryabkin V.A., Sokolov Yu.I., Sorokina N.I. and Shuvalov L.A., *Kristallografiya*, **26**, 1259 (1981).
3. Sorokina N.I., Muradyan L.A., Loshmanov A.A., Fykin L.E., Rider E.E., Dobrzhansky G.F. and Simonov V.I., *Kristallografiya*, **29**, 220 (1984).
4. Puchkovskaya G.A. and Tarnavski Yu.A., *J. Mol. Struct.*, **267**, 169 (1992).
5. Puchkovskaya G.A. and Tarnavski Yu.A., *Ukr. Fiz. Zhurnal*, **38**, 770 (1993).
6. Puchkovskaya G.A. and Tarnavski Yu.A., *J. Mol. Struct.*, **403**, 137 (1997).
7. Nakamoto K., *Infrared and Raman Spectra of Inorganic and Coordination Compounds.* John Wiley and Sons, NY, 1986.
8. Barabash A., Gavrilko T., Puchkovskaya G., Eshimov K. and Yaremko A., *Kristallografiya*, **34**, 663 (1989).
9. Barabash A., Gavrilko T., Eshimov K., Puchkovskaya G. and Shanchuk A., *J. Mol. Struct.*, **294**, 61 (1993).
10. Novak A., *Structure and Bonding*, **18**, 177 (1974).
11. *The Hydrogen Bond. Recent developments in theory and experiments* (Ed. P. Schuster *et al.*). North-Holland, 1976.
12. Engelen B., Gavrilko T., Panthofer M., Puchkovskaya G. and Sekirin I., *J. Mol. Struct.*, **523**, 163 (2000).
13. Ichikawa M., *Acta Cryst*., *Sect. B*, **34**, 2074 (1978).
14. Barabash A.I., *J. Mol. Struct.*, **270**, 517 (1992).
15. Baisa D.F., Barabash A.I., Shadchin E.A., Shanchuk A.I. and Shishkin V.A., *Kristallografiya*, **34**, 1025 (1989).